第 27 卷 第 6 期
2013 年 12 月

实 验 流 体 力 学
Journal of Experiments in Fluid Mechanics

Vol. 27, No. 6
Dec., 2013

文章编号：1672-9897(2013)06-0064-07

Application of electrostatic probe method for electron density measurement in hypersonic ionized flows

WANG Qiu, ZHAO Wei, YU Xi-long, JIANG Zong-lin

(State Key Laborotary of High Temperature Gas Dynamics, Institute of Mechanics, CAS, Beijing 100190, China)

Abstract: A laboratory measurements program has been performed in the JF-10 high enthalpy shock tunnel, which provides the aerodynamic and aerothermal conditions wherein plasma environment issues can be quantitatively examined. Electron number density is measured by a swept-voltage electrostatic probe placed on a 10 degree wedge model. Dual-cable method is explored in order to reduce the induced noise due to the RC characteristic of coaxial cables when a high frequency swept voltage is applied to the probe. Results show that electron density in the boundary layer of the model can be effectively acquired and the dual-cable method turns out to be an effective way for electron density measurement in the short duration test facilities.

Key words: electrostatic probe; electron density; hypersonic; high enthalpy shock tunnel

高超声速电离绕流中电子密度的静电探针测量方法研究

汪 球，赵 伟，余西龙，姜宗林

（中国科学院力学研究所 高温气体动力学国家重点实验室，北京 100190）

摘要：高焓激波风洞是开展高超声速电离绕流研究的重要地面模拟设备。在中科院力学所 JF-10 高焓风洞上通过新的破膜技术获得了稳定运行的试验状态，利用施加高频扫描电压的静电探针来探索模型边界层内的电子密度测量方法研究。为解决高频扫描时线路由于 RC 特性所带来的噪音干扰问题，针对测试环境发展了新的探针电路。结果表明：新型探针电路大大降低了线路干扰噪音，能够有效测量模型边界层内的电子密度分布规律。

关键词：静电探针；电子密度；高超声速；高焓激波风洞

中图分类号：O242　　文献标识码：A

0 Introduction

As we know, aerodynamic processes cause density and temperature gradients in the non-planar flow field behind a bow shock, and aerothermal processes arouse plasma phenomena as a result of thermal ionization. The characteristics of the electron component of the high temperature plasma formed around a hypervelocity reentry vehicle play a dominant role in determining the radar characteristic and radio wave propagation characteristic of the vehicle[1-2]. For this reason, research on electron density distribution in hypersonic ionized flows is really necessary[3-4].

The high enthalpy shock tunnel, one of the most widely used hypersonic flow simulation ground facilities, is capable of generating certain aerodynamic and aerothermal conditions wherein plasma environment issues can be quantitatively examined. The electrostatic probe, which has the qualities of wide dynamic range, simple instrumentation and good spatial resolution, is a well-known and widely used diagnostic tool for measuring electron temperature and density[5-6]. In order to deduce these two plasma parameters, an I-V characteristic curve has to be generated by sweeping the probe voltage. Considering the fact that the effective test time of a high enthalpy shock tunnel is only several milliseconds, the

Received date: 2013-01-16; **Revised date**: 2013-06-20

Foundation item: National Natural Science Foundation of China (90916028) and the Knowledge Innovation Program of the Chinese Academy of Science (KJCX2-EW-L05)

swept voltage frequency applied to the probe should be over 1kHz. However, due to the RC characteristic of coaxial cables, an induced noise will appear when a high frequency swept voltage is applied. Such a noise is very annoying and difficult to remove, particularly when the probe signal is weak [7-9].

In this paper, a stagnation enthalpy of 16.2MJ/kg is generated in the JF-10 high enthalpy shock tunnel at LHD, Institute of Mechanics, Chinese Academy of Sciences. The electron density in the ionized boundary layer of a 10 degree wedge model is measured using an electrostatic probe. And a dual-cable circuit is used to reduce the induced noise originated from the high frequency swept voltage. Results show that the noise reduction method is effective and the electron density can be completely acquired. The combination of a high enthalpy shock tunnel and electrostatic probe can play an important role in the experimental research of plasma diagnostics.

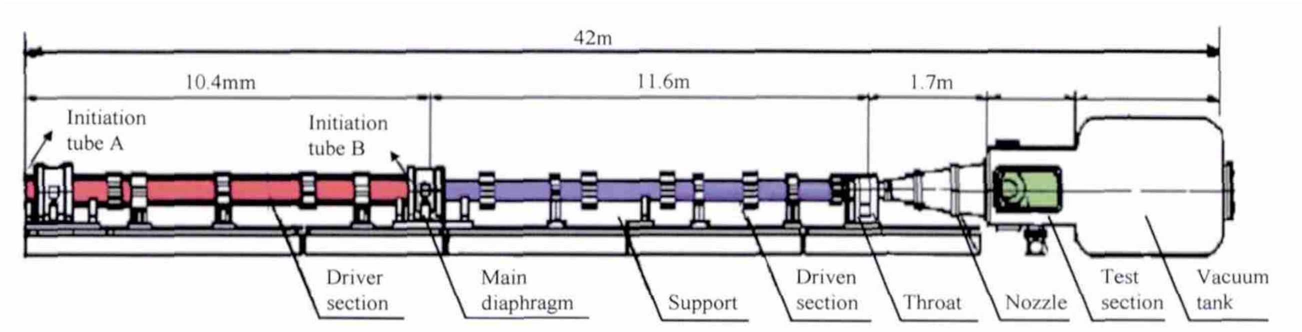

Fig. 1 Sketch of the JF-10 detonation shock tunnel
图 1 JF-10 高焓激波风洞结构示意图

1 Experimental descriptions

1.1 Experimental facilities

The sketch of JF-10 detonation high enthalpy shock tunnel is shown in Fig. 1. It is 42m in total length, the detonation driver chamber has an inner diameter of 150mm, and that of the driven shock tube is 100mm. A conical nozzle is used in the experiment, with the throat diameter of 11mm and the exit diameter of 500mm. Using the detonation product gases at high temperature and pressure as the driver gases, the test flow with high enthalpy and high pressure can easily be acquired. A large number of theories, experiments and numerical simulations have provided reliable foundation for its working principle and driving performance. Air quality and test time are also constantly improved[10-13].

1.2 Test Conditions

In order to burst a metal diaphragm without its fragmentation under the downstream operation mode, dual ignition system is used in the experiment. The initiation tube A is first ignited. Then the initiation tube B is ignited by a delay controller before the arrival of detonation wave at the primary diaphragm position. The delay time is specified depending on the detonation chamber length and the detonation wave speed. The experimental results show that the dual ignition system has greatly improved the stability and repeatability of the test condition, which provides powerful support for the conducting of the experiments. Typical stagnation pressure history is shown in Fig. 2. The plateau pressure maintains more than 10 milliseconds, but the effective test time is about 5 milliseconds considering the total amount of test gas. However, the test time is enough for our measuring system, which also brings much convenience for the design of models.

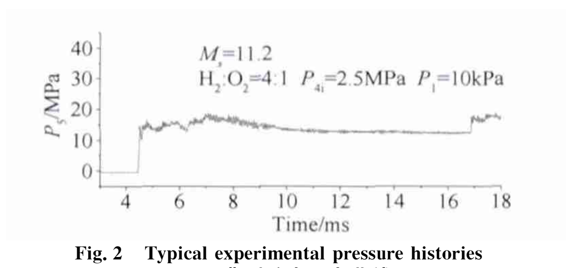

Fig. 2 Typical experimental pressure histories
图 2 典型驻室压力曲线

The stable operation parameters of the test condition are shown in Table 1. "M_s" represents the primary shock wave Mach-Number in the shock tube, which is obtained through ionization probes distributed on the shock tube and the reservoir conditions of the shock tunnel are then calculated. According to the definition of the conventional shock tunnel terminology, subscript "4i" and "1" represent the initial condition in the detonation chamber and that in the driven section, respectively. Subscript "0" represents the reservoir condition. The experiment is carried out at the initial pressure of 2.5 MPa in the driver chamber, with the H_2/O_2 mixture ratio of 4∶1.

Together with the probe size, the free-stream flow parameters would determine whether the free-molecular, transitional, or collisional sheath considerations would have to be invoked for proper data reduction. Pitot rake has been used to calibrate the free-stream flow. However, we can't determine all the free-stream flow parameters of a high enthalpy shock tunnel just from the pitot pressure and the reservoir conditions like in conventional wind tunnels. Because of high temperature effects, the free-steam flow of the high enthalpy shock tunnel is in a state of thermal-chemical non-equilibrium. A thermo-chemical non-equilibrium program is used to determine the free-stream flow parameters, which are shown in table 1[14]. The nozzle exit velocity exceeds 5000m/s, in which high temperature phenomena can be experienced by the test gas. "Ma" represents the free-steam Mach-Number in the test section.

Table 1 Test conditions and free stream parameters
表 1 试验状态及自由流参数

Initial conditions			Stagnation conditions					Free-stream conditions			
H_2∶O_2	P_{4i}/MPa	P_1/kPa	M_s	P_0/MPa	T_0/K	H_0/(MJ·kg^{-1})	P/Pa	T/K	ρ/(kg·m^{-3})	U/(m·s^{-1})	Ma
4:1	2.5	10	11.2	17.9	7890	16.2	103	430	7.5×10^{-4}	5086	11.7

1.3 Test model description

The test model used in the experimental study is a 10-deg wedge model made of steel. Five probes in a group at one place, perpendicular to the wall surface, with a distance of 4mm between each other, are used to measure the electron density distribution in the boundary layer or the shock layer. The probes are 300mm from the front. Sketch of the model is shown in Fig. 3 and the experiment is conducted with no angle of attack

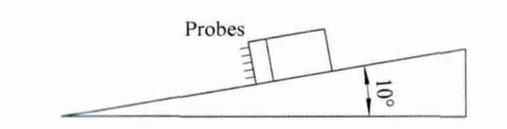

Fig. 3 The sketch of the test model and probes distribution
图 3 试验模型及传感器分布示意图

2 Dual-cable method and probe theory

2.1 Dual-cable method

A cylindrical electrostatic probe with a radius of 0.15mm and a length of 8mm is used. For data acquisition, BNC coaxial cables with the length of several meters are necessary to connect the probe and the computer acquisition system. Due to the RC characteristics of the coaxial cables, induced noise will appear under the high frequency sweeping voltage, which is almost of the same order of magnitude as the probe signals in the wind tunnel. Such a noise is very annoying and difficult to remove.

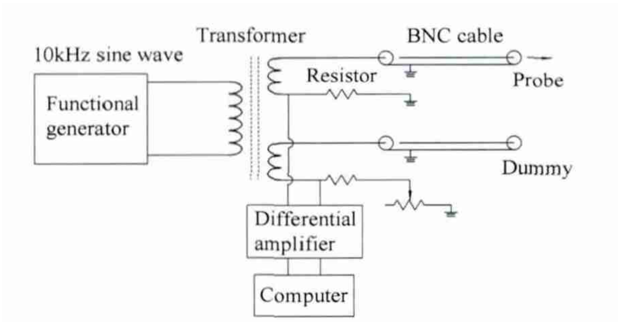

Fig. 4 A dual-cable probe circuit
图 4 探针扫描电路

In order to reduce the noise, a dual-cable method is used, where the lead capacitance is compensated for by subtracting out the signal from a dummy cable of equivalent length. The schematic of the measuring circuit is shown in Fig. 4. A sine probe voltage is generated by a functional generator (AFG 3101). Two secondary windings from the transformer provide power supply for the active probe and the dummy probe, respectively. The cables of the two probes are of the same type, are equal in length, and are tied together. A fixed step resistor and a variable wire resistor are connected to the dummy coaxial cable, which can provide fine tuning by the course adjustment. After being tuned, the induced noises of the two cables are nearly identical.

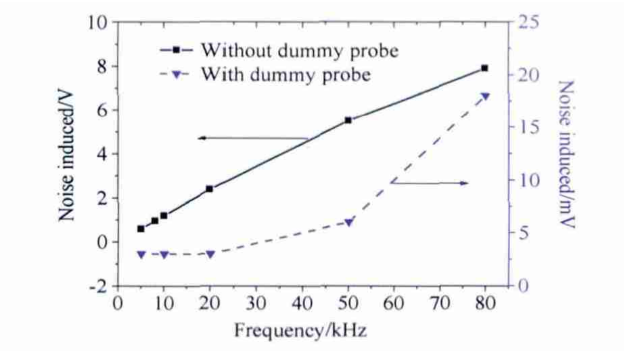

Fig. 5 The amplitude of the induced noises as a function of the sweeping frequency of the applied sine voltage

图 5 噪音随扫描频率变化曲线

In Fig. 5, the amplitude of the induced noises as a function of the sweeping frequency is shown, where the sine voltage is used. Considering the fact that the test time of the high enthalpy shock tunnel is several milliseconds, the sweeping frequency should be over 1kHz. Without the dummy probe, the induced noise would be 1V or more, which is almost of the same order of magnitude as the probe signal. Instead, the induced noise would be less than 5mV after being tuned with a dummy probe, which is negligible when the sweeping frequency is below 50kHz. The frequency is set to be 10kHz in our experiment.

2.2 Probe theory

Electrostatic probe, which has wide dynamic range, simple instrumentation and good spatial resolution, has long been used as a fundamental diagnostic tool for measuring the properties of plasma. Basically an electrostatic probe consists of a conducting metal surface to act as the sensor, a voltage supply, and a current measuring device. Although electrostatic probes are relatively simple devices, the theory underlying the probe response is, unfortunately, complicated, which is mainly determined by the influence of the probe electrode dimensions on the plasma properties. Whether the free-molecular, transitional, or collisional sheath considerations would have to be invoked for proper data reduction mainly depend on three parameters, the probe radius R, the mean free paths of the charged particles λ_{ei}, and the Debye length λ_D. The major disadvantage of the electrostatic probe is that it is an intrusive measurement technique, which may disturb the plasma flow. However, this undesirable aspect can be minimized by keeping the probe size small. In our experiment, a cylindrical electrostatic probe with a radius of 0.15mm and a length of 8mm is used. It minimized the disturbance of the probe to the flow and the collisionless near free-molecular probe theory is suitable. Considering the high temperature and high speed gas flow, the probe material is chosen to be iridium, which can provide enough strength and anti-oxidation protection. And the probe is oriented so that it is always aligned with the flow direction during the experiment.

A sine swept voltage is applied to the probe, over a voltage range from -10V to 10V, which is sufficient to record both the ion saturation region and the electron retarding field region of the probe characteristic. Probe data reduction follows the theory of Laframboise[17] for the case of a collisionless sheath, which gives the ion current density j_i to a single probe aligned with the plasma:

$$I_i = Aen_e\sqrt{\frac{kT_e}{2\pi m_i}}\,i_+\left(\chi_p, \frac{T_i}{T_e}, \frac{R}{\lambda_D}\right) \quad (1)$$

wherein, T_i is the ion temperature. m_i is the ion mass, which can take the mass of NO^+ in the experiment. I_i is the measured ion current, which is $I_i = j_i \cdot A$, A is the probe surface area. χ_p is the nondimensional probe potential:

$$\chi_p = \frac{e}{kT_e}(V_p - V_\infty) \quad (2)$$

χ_p shows the dimensionless difference between the probe potential V_p and the plasma potential V_∞. V_∞ is the potential at which the probe collects both ions and electrons (random currents) without the aid of electric fields. i_+ is a normalization factor, which is a function of χ_p, the ratio of ion to electron temperature, and the ratio of probe radius to Debye length. The correction factor can be set to 1 in good approximation if the ratio of probe radius to Debye length is greater than 50[18].

When the voltage applied to the probe is swept from negative toward positive values, $\chi_p \to 0$ and the electron current collected by the probe increases rapidly because the higher thermal velocities of the electrons enable them to reach the probe surface in spite of the repelling voltage. This region of the probe characteristic is called the retarding field region. In the retarding region:

$$I_e = Aen_e\sqrt{\frac{kT_e}{2\pi m_e}}\exp(\chi_p) \quad (3)$$

Differentiating the equation (3) we can get:

$$\frac{\mathrm{dln}(j_e)}{\mathrm{d}V_p} = \frac{e}{kT_e} \quad (4)$$

From equation (4), the electron temperature T_e can be obtained by plotting the slope of the logarithmic electron current in the retarding region versus the probe potential. Then n_e can be determined by T_e from equation (1).

3 Results and discussion

Five probes are installed in a common rake, with each probe aligned with the local flow direction and positioned at different distances off the vehicle surface so as to measure the electron density profile through the boundary layer. A sine swept voltage is applied to the probes, over a voltage range from -10V to 10V, and the sweeping frequency is 10kHz. Considering the fact that the effective test time of the tunnel is over 2ms, a repetition of more than 20 times of I-V probe characteristics can be acquired for a probe in one test.

Fig. 6 (a) shows the original signals of the 10kHz sine swept voltage and the probe current during the effective test time. Fig. 6(b) is a typical I-V characteristic curve, which is derived from one cycle of Fig. 6(a). V_F is the floating potential, at which no net current is drawn since the ion current I_i equals to the electron current I_e. V_F can be defined from the probe characteristic with precision. But the plasma potential V_∞, which has fluctuations, can't be determined with precision. The point where $\mathrm{d}I/\mathrm{d}V_P$ is maximum is set to be the plasma potential. The curve range between V_F and V_∞ is called the electron retarding region, from which the electron temperature is derived. When the negative probe potential is sufficiently large in magnitude with respect to the plasma potential, only ions will be collected and all electrons are repelled from the probe. Due to the typically large masses, and hence low mobility of the ions in plasma, the current is measured to be small and negative. The trace will exhibit a plateau in current, dubbed as the ion saturation region, which is shown in Fig. 6(b). Together with the probe size information, the electron temperature and density can be obtained from the I-V characteristic curve. The theory and method are presented in section 2.2.

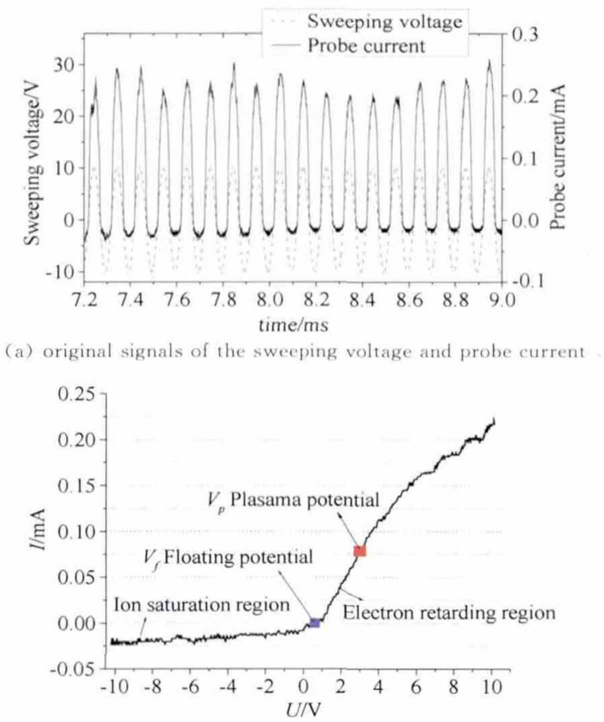

(a) original signals of the sweeping voltage and probe current

(b) typical I-V characteristic curve

Fig. 6 Electric probe signals

图 6 探针扫描电压和探针电流信号及典型伏安特性曲线

Fig. 7 shows the electron density profiles for the test runs of No. 1 and No. 2. These test runs represent repeated data for the 0-deg AOA, which shows good repeatability. The maximal density is about $7\times10^{11}/\mathrm{cm}^{-3}$ at the test point 4mm close to the wall, and it decreases with the increase of the distance from the wall. However, the distance above the surface for the peak level is not very discernible at this point, since the density may be larger than $7\times10^{11}/\mathrm{cm}^{-3}$ at the place closer to the wall. On the whole , however, the dual-cable method turns out to be an effetive way for electron density measurement in the hypersonic ionized flows in high enthalpy shock tunnel. More probes will be used and more experiments will be conducted later.

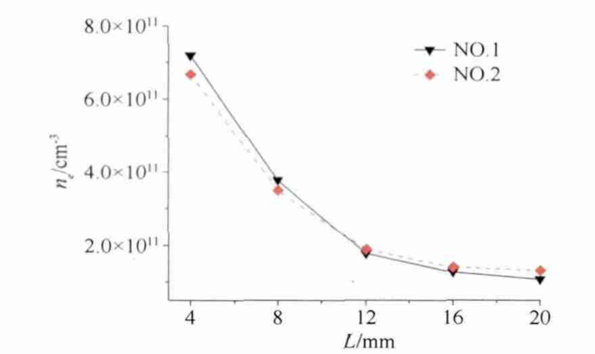

Fig. 7 The electron density distribution perpendicular to the wall
图 7 垂直壁面方向电子密度分布

4 Conclusion

A laboratory measurements program has been performed in the JF-10 high enthalpy shock tunnel, and the electron density in the hypersonic ionized flows with the presence of a 10 degree wedge model has been measured. The results show that：

(1) A stable test flow with stagnation enthalpy of 16.2MJ/kg is generated in the JF-10 high enthalpy shock tunnel using the dual ignition system, which provides the aerodynamic and aerothermal conditions wherein plasma environment issues can be quantitatively examined.

(2) The dual-cable method is explored, which can obviously reduce the induced noise when a high frequency swept voltage is applied to the electrostatic probe.

(3) Electron density can be effectively acquired using the dual-cable method and the data exhibited good repeatability.

Acknowledgement：

The authors would like to acknowledge the National Natural Science Foundation of China (90916028) and the Knowledge Innovation Program of the Chinese Academy of Science (KJCX2-WE-L05). The authors thank Li Zhongfa and Fang Zhijia for their kind assistance in experiments.

References：

[1] KAZUHISA Fujita, SUNICHI Sato, TAKASHI Abe. Electron density measurements behind strong shock waves by H-β profile matching[J]. Journal of Thermophysics and Heat Transfer, 2003, 17(2): 210-216.

[2] DALLAS T Hayes. Electrostatic probe measurements of flow field characteristics of a blunt body reentry vehicle[R]. AIAA 72-694, 1972.

[3] MA Ping, ZENG Xue-jun, LIU Seng, et al. Experimental research of wake electron density of hypersonic sphere models[J]. Journal of Experiments in Fluids Mechanics, 2010, 24(1): 20-25.

[4] LIAO Guang, LIN Zhen-bin, GUO Da-hua, et al. Measurement and diagnosis of the wake electron density in high enthalpy wind tunnel[J]. Journal of Experiments in Fluids Mechanics, 2010, 24(5): 79-82.

[5] MENART J, SHANG J, HAYES J. Development of a Langmuir probe for plasma diagnostic work in high speed flow[R]. AIAA 2001-2804, 2001.

[6] PAUL M Chung. Weakly ionized nonequilibrium viscous shock-layer and electrostatic probe characteristics[J]. AIAA Journal, 1965, 3(5): 817-825.

[7] YANG T F, ZU Q X, LIU Ping. A dual-cable noise reduction method for Langmuir probes[J]. Review of Scientific Instruments, 1995, 66(7): 3879-3882.

[8] ROBERT B. Lobbia, MICHAEL J. Sekerak, RAYMOND Liang, et al. High-speed dual Langmuir probe measurements of the plasma properties and EEDFs in a HET plume[C]. The 32nd International Electric Propulsion Conference, Wiesbaden, Germany, 2011.

[9] LOBBIA R. Gallimore. High-speed dual langmuir probe[J]. Review of Scientific Instruments, 2010, 81(7): 073503.

[10] YU Hong-ru, ZHAO Wei, YUAN Sheng-xue. Performance of Shock tunnel with H_2-O_2 detonation driver[J]. Aerodynamic Experiment and Measurement & Control, 1993, 7(3): 38-42.

[11] YU Hong-ru. Oxyhydrogen combustion and detonation driven shock tube[J]. Acta Mechanica Sinaca, 1999, 15(2): 97-107.

[12] JIANG Zong-lin, ZHAO Wei, WANG Chun. Forward-running detonation drivers for high-enthalpy shock tunnels[J]. AIAA Journal, 2002, 40(10): 2009-2016.

[13] ZHAO Wei, JIANG Zong-lin, SAITO T, et al. Performance of a detonation driven shock tunnel[J]. Shock Waves, 2005, 14: 53-59.

[14] ZENG Ming. Numerical rebuilding of free-stream measurement and analysis of nonequilibrium effects in high-enthalpy tunnel[D]. Institute of Mechanics, Chinese Academy of Sciences, 2007.

[15] KENNETH M. Chadwick. Plasma and aerothermal measurements on a hypervelocity re-entry vehicle[J]. Journal of Spacecraft and Rockets, 1997, 34(5): 602-608.

（下转第 85 页）

[14] LV Zhi-guo, LI Guo-jun, ZHAO Rong-juan, et al. The development of piezoelectric skin friction balance for shock tunnel[C]. The 8th International Symposium on Strain-Gauge Balances, 2012.
[15] WOODEN P, HULL G. Correlation of measured and theoretical heat transfer and skin friction at hypersonic speeds, including Reynolds analogy[R]. AIAA 90-5244.
[16] DAVID M Hazelton, RODNEY D W Bowersox. Skin friction correlations for high enthalpy flows[R]. AIAA-98-1636.
[17] 陈懋章. 粘性流体力学基础. 研究生教学用书[M]. 北京:高等教育出版社, 2002.
[18] GOYNE C P, STALKER R J, PAULL A. Shock-tunnel skin-friction measurement in a supersonic combustor [J]. Journal of Propulsion and Power, 1999, 15(5): 699-705.
[19] DAVID M Hazelton, RODNEY D W Bowersox. Heat transfer and skin friction in a Mach 6 inlet flow[R]. AIAA 99-4890.
[20] BRENDA M Kulfan. Assessment of CFD predictions of viscous drag[R]. AIAA-2000-2391.
[21] 李中华, 吕治国, 王刚. 0.6m 激波风洞高升阻比标模测力试验不确定度分析[R]. 国防科技报告. 四川绵阳: 中国空气动力研究与发展中心, 2011.
[22] 陈作斌. 风洞试验质量评估[R]. 译自 AGARD AR-304. 四川绵阳: 中国空气动力研究与发展中心, 1995.

作者简介：

吕治国(1963-), 男, 高级工程师, 硕士。研究方向: 高超声速脉冲设备研究激波风洞气动力及相关试验技术。通讯地址: 四川省绵阳市中国空气动力研究与发展中心(621000), 联系电话: 0816-2465790, E-mail: lzgde2003@126.com

(上接第 69 页)

[16] HARALD A Habiger, MONIKA Auweter-Kurtz. Investigation of a high enthalpy air plasma flow with electrostatic probes[R]. AIAA 96-1864.
[17] LAFRAMBOISE J G. Theory of spherical and cylindrical Langmuir probes in a collisionless Maxwellian plasma at rest[R]. Univ. of Toronto Inst. For Aerospace Studies, 1966.
[18] SONIN A A. Free-molecule Langmuir probe and its use in flowfield studies[J]. AIAA Journal, 1966, 4(9): 1588-1596.

Author biography:

WANG Qiu (1985-), male, born in Huanggang city, Hubei province, doctor. Research direction: high enthalpy flow and high temperature gas dynamics. Mail address: State Key Laboratory of High-temperature Gas Dynamics, Institute of Mechanics, Chinese Academy of Sciences, No. 15 West Beisihuan Road, Beijing 100190, China. Telephone: 010-82543845, E-mail: wangqiu@imech.ac.cn